

引用格式: WANG Bin, SUN Degui, SHANG Hongpeng. Investigation for Relationship between Sidewall Roughness of Silicon-on-insulator Waveguide and Loss of Guided-mode[J]. Acta Photonica Sinica, 2021, 50(5):0506005
王彬,孙德贵,尚鸿鹏. 绝缘体上硅波导侧壁粗糙度与模式损耗的相关性[J]. 光子学报, 2021, 50(5):0506005

绝缘体上硅波导侧壁粗糙度与模式损耗的相关性

王彬,孙德贵,尚鸿鹏

(长春理工大学 理学院, 长春 130022)

摘 要: 绝缘体上硅光波导侧壁粗糙度引起的光损耗是限制硅基集成线路被广泛应用的重要因素之一, 利用激光扫描共聚焦显微镜精确测量了 SOI 波导各相异性分布的侧壁粗糙度, 进而将一个三维侧壁粗糙度引入到光波导传输损耗计算的传统理论模型中, 获得了更加精确的模型。数值模拟表明, 侧壁粗糙度与波导结构决定的相关长度与侧壁粗糙度对光传输损耗产生同步影响。用法布里-珀罗(F-P)腔调制谐振输出方法测量光波导传输损耗, 测量结果与数值计算结果非常吻合, 说明各相异性粗糙度分布的测量精度及其引起的光传输损耗的理论模型具有很高的可信度。一条 4 μm 脊宽 SOI 波导, 当侧壁粗糙度在水平和垂直方向的平均值分别为 22 nm 和 23 nm 时, 对于 TE-和 TM-模式, 计算获得的传输损耗均为 4.5~5.0 dB/cm, 实验获得的平均光传输损耗为 4.3 dB/cm。本文研究结果与结论对 SOI 光波导器件的研究与开发具有参考价值。

关键词: 绝缘体上硅波导; 侧壁粗糙度; 相关长度; 光传输损耗; 光损耗测量

中图分类号: TN256

文献标识码: A

doi:10.3788/gzxb20215005.0506005

Investigation for Relationship between Sidewall Roughness of Silicon-on-insulator Waveguide and Loss of Guided-mode

WANG Bin, SUN Degui, SHANG Hongpeng

(School of Science, Changchun University of Science and Technology, Changchun 130022, China)

Abstract: The optical loss caused by Waveguide Sidewall Roughness (SWR) of Silicon-on-insulator (SOI) is one of the restrictions to the adoptions of silicon photonic integrated circuits. In this paper, the anisotropic SWR of an SOI waveguide is measured by Conformal Laser Scanning Microscope (CLSM) and with introduction of a Three-dimensional (3D) anisotropic SWR, the traditional theoretical model for defining the Optical Propagation Loss (OPL) coefficient, so that a more accurate theoretical model is obtained. Numerical simulations show that the waveguide structure determined Correlation Length (CL) and the SWR have the synchronous effects on the OPL. Fabry-Perot (F-P) cavity modulation resonance output is used to accurately measure the OPL, and the measured values are agreeable with the simulation result, implying the improved model has more believability. For a waveguide with a 4 μm width, when the average horizontal and vertical SWR values are 22 nm and 23 nm, respectively, the simulation results of OPL coefficient for both TE- and TM-mode are 4.5~5.0 dB/cm, while the experimental result is 4.9 dB/cm.

Foundation item: Talent Plan Fund of Jilin Provincial Human Resources and Social Security (No. 634190874002), Natural Science Foundation of Jilin Province/China (No. 20180101223JC), Human Resources and Social Security Talent Plan Fund of Jilin Province (No. 634190874002), Natural Science Foundation of Jilin Province (No. 20180101223JC)

First author: WANG Bin (1993—), male, M.S. degree candidate, mainly focuses on silicon-based optical waveguide device. Email: dawwangbin123@163.com

Corresponding author: SUN Degui (1960—), male, professor, Ph. D. degree, mainly focuses on integrated photonics device technology. Email: sundg@cust.edu.cn

Received: Nov.11, 2020; **Accepted:** Mar.1, 2021

<http://www.photon.ac.cn>

Hence, the outcomes and conclusion obtained are very valuable to be referred for research and development of SOI waveguide devices.

Key words: SOI waveguide; Sidewall roughness; Correlation length; Optical propagation loss; Measurement of optical loss

OCIS Codes: 060.4510; 230.7370; 240.6700; 290.5825; 240.5770; 220.4840

0 Introduction

Optical Propagation Loss (OPL) is the core problem of Silicon-On-Insulator (SOI) optical waveguide devices, and the main source of the OPL is the inevitable Sidewall Roughness (SWR) caused by the waveguide fabrication processing^[1-2]. With the development and applications of SOI optical waveguide photonic integrated devices in the past few years, enormous research efforts in this area have been made in the calculation of waveguide OPL, an obvious trend is that the original two-dimensional (2-D) waveguide structure is moved to the understanding to the three-dimensional (3-D) roughness distribution, including the paper we just published, the calculation model is gradually improving the Payne-Lacey (PL) model^[3].

The currently accepted theoretical model for the relationship between the waveguide SWR and the light guided mode is the PL theoretical model that was proposed by PAYNE F P and LACEY J P R in 1994^[4]. Since then, the PL theoretical model has been widely employed to study the Optical Propagation Loss (OPL) and some improvements have been carried out^[5-7]. Typically, in 2005, BARWICZ T and HAUS H A carried out their theoretical work based on the 3-D interaction between the polarized Poynting vector and the Vertical Shape of the Field (VSF) so that they could give rise to more detailed simulations of the OPL values of both the low and high index-contrast waveguides^[5]. In 2006, POULTON C G et al. gave a more powerful explanation that the OPL caused by the SWR is from the two conversions: the conversion from a guided-mode to a radiation mode and the conversion from the radiation mode to a leaky mode, so that they could accurately compute the electric fields with the Finite Difference Time-domain (FDTD) method^[6]. Especially for the SOI waveguides, in 2008, SCHMID J H et al. employed the non-uniform waveguide boundaries to study the scattering loss^[7], and in 2009 YAP K P et al. studied the correlation among the light scattering loss, the sidewall roughness and channel width of the SOI waveguides^[8]. Since 2019, we have introduced the Confocal Laser Scanning Microscope (CLSM) into the measurement technology of waveguide SWR and obtained the 3-D distribution properties of silicon dioxide and SOI waveguides^[3,9-10]. In our previous work, both the improved theoretical model and the latest roughness test results show that the correlation length determined by the waveguide structure plays a key role in causing the light propagation loss, but not much attention has been paid to it.

In this article, the improved theoretical model of defining the OPL coefficient on the SWR is exploited where the components of the SOI waveguide SWR at horizontal and vertical direction are introduced. Then, the measured values of 3-D distributed waveguide SWR are obtained with the CLSM technique. As a result, with such a combinative model, the dependences of the optical propagation loss coefficient of the waveguide on the SWR distribution and the width are systematically simulated. Finally, the great agreements between the numerical simulation results based on the measured SWR values and the experimental results are achieved.

1 Device structure and concepts

1.1 Device concepts and theoretical models for the OPL caused by SWR

Fig. 1 shows a schematic 3-D configuration of a straight waveguide in which the waveguide core has a refractive index of n_1 and a channel width of $2d$, and the cladding material has a refractive index of n_2 , and the effective index of the guided-mode is N_{eff} . If the wavelength of the light wave in air is λ , with the wave number $k_0 = 2\pi/\lambda$ and the Finite Difference Processing of Beam Propagation Method (FD-BPM), the effective index N_{eff} of a single guided-mode is obtained, and further based on the propagation constant of this guided-mode $\beta = k_0 \cdot N_{\text{eff}}$, three dimensionless parameters h , V and p of guided-mode defined by the PL model can be defined as^[3-4]

$$(h, V, p) = \left(d\sqrt{n_1^2 k_0^2 - \beta^2}, \quad k_0 d\sqrt{n_1^2 - n_2^2}, \quad d\sqrt{\beta^2 - n_2^2 k_0^2} \right) \quad (1)$$

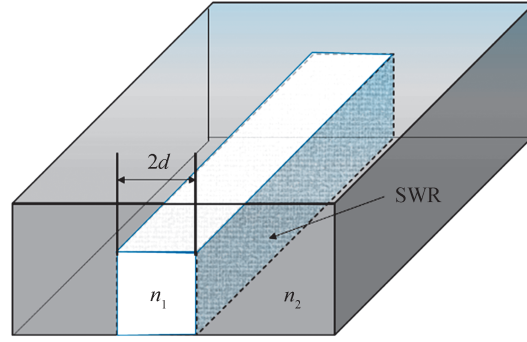


Fig. 1 Perspective view of a schematic SOI waveguide

where h and p are the parameters defining the guided mode field in the literature on optical waveguides^[11, 12], V is the product of three elements, $\sqrt{n_1^2 - n_2^2}$ is the numerical aperture of a symmetric planar waveguide, d is half width of the waveguide core, leading to the other dimensionless parameters as

$$(\Delta, x, \gamma) = \left((n_1^2 - n_2^2) / (2n_1^2), p(L_c/d) p(L_c/d), (n_2 V) / (n_1 p \sqrt{\Delta}) \right) \quad (2)$$

Consequently, for both the TE-like and TM-like modes, the SWR induced optical scattering loss is related to both the y - and z -components of roughness, so the dependences of the optical intensity loss coefficients α_{3D} (TE/TM) on the 3-D SWR σ_{3D} (TE/TM) can be expressed as^[3]

$$\alpha_{3D}(\text{TE/TM}) = 4.34 \left(\frac{\sigma_{3D}^2(\text{TE/TM})}{\sqrt{2} d^4 \beta_{\text{TE/TM}}} g(V) \cdot f_e(x, \gamma) \right) \quad (3)$$

where α_{3D} (TE/TM) is the SWR defined in the 2-D form and the loss coefficient is in dB/cm, the functions $g(V)$ is defined as

$$g(V) = \frac{h^2 V^2}{1 + p^2} \quad (4)$$

and $f_e(x, \gamma)$ is defined as

$$f_e(x, \gamma) = \frac{\{[(1+x^2)^2 + 2x^2\gamma^2]^{1/2} + 1 - x^2\}^{1/2}}{[(1+x^2)^2 + 2x^2\gamma^2]^{1/2}} \quad (5)$$

where transferring functions, $f_e(x, \gamma)$ is used to determine the correlation length L_c with the parameters x and γ at the peak value.

1.2 Determination of the Correlation Length L_c

The numerical simulation for the function $f_e(x, \gamma)$ is shown in Fig. 2, where the peak position indicates the maximum autocorrelation value. So, the corresponding values of x and γ play the role of making $f_e(x, \gamma)$ have the maximum autocorrelation effect, and then the corresponding L_c value calculated from Eq. (2) is the correlation length value of this waveguide.

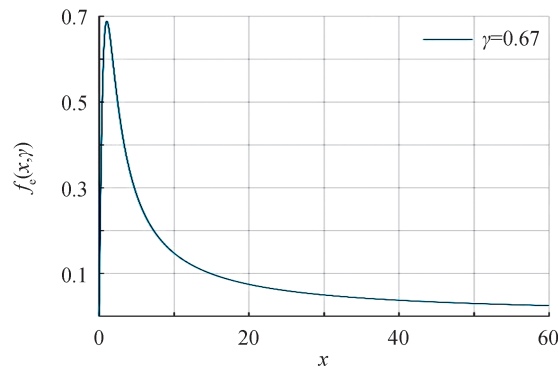


Fig. 2 Illustrative plot of $f_e(x, \gamma)$ vs the variable x for determining L_c

2 Numerical simulations of optical propagation loss

2.1 Numerical simulations for variables x and γ of the function $f_e(x, \gamma)$

With Eq. (4), the numerical simulation results of two key variables x and γ of the function are obtained as shown in Figs. 3(a) and 3(b), respectively. From Fig. 3(a), we find that the variable x is strongly dependent on the refractive index of the SOI waveguide core, but it is weakly dependent of the rib width. Illustratively, all the five curves are very close to one another, namely, when the core refractive index is changed from 3.43 to 3.48, almost all the five x values are decreased from 1.6913 to 1.6885. For the simulation results of variable γ are almost the same as the case of x . For instance, γ is also weakly dependent of the rib width, so all the five curves are very close to one another, namely, when the core refractive index is changed from 3.43 to 3.48, almost all the five γ values are decreased from 0.673 to 0.662. The comparison between Figs. 3(a) and 3(b) also shows that corresponding to the effective index change, the relative change of x is only 0.17%, while the relative change of γ reaches 1.63%. In summary, γ has the much stronger dependence on the refractive index of SOI waveguide core than x , but they are almost independent of the rib width.

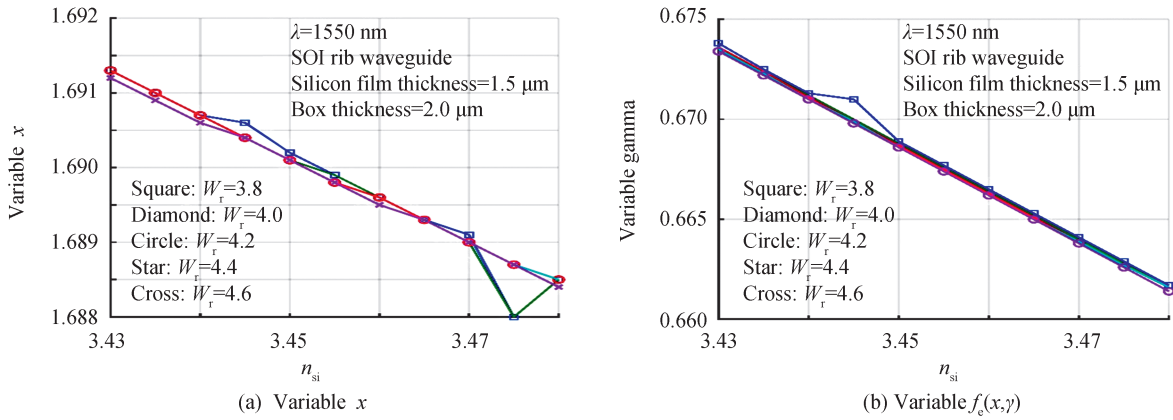


Fig. 3 Numerical simulations for the dependences of functional variables of x and $f_e(x, \gamma)$ on the waveguide structures

2.2 Numerical simulations for the correlation length L_c on the waveguide structure

With the simulation results of x and γ shown in Figs. 3(a) and 3(b), respectively, with Eq. (4), the plot of function $f_e(x, \gamma)$ versus variable x for each waveguide structure is carried out and then the value of the correlation length L_c of this waveguide structure is obtained. Further, for the possible waveguide structures that can create single-mode operations, the corresponding distributions of L_c are obtained with respect to five values of channel width W , as shown in Fig. 4.

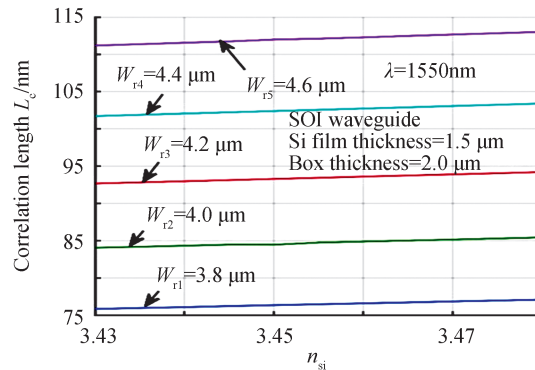


Fig. 4 Numerical simulations for the dependences of L_c on the waveguide structures

Note that the dependences of L_c on the two waveguide parameters: the rib width and the core refractive index are inverse to the cases of the two variables x and γ . Namely, L_c has no big change with the core refractive index, but all the five lines of L_c values are dramatically different from one another, namely, it

strongly dependent on the rib width of the SOI waveguide. Eqs. (1) ~ (3) show that the OPL coefficient α_{3D} is related to both L_c and W_r (i.e., $2d$), so these two parameters of waveguide: n_1 and $2d$ have great impacts upon the SWR-caused OPL.

3 Measurements for the anisotropic SWR and the OPL

3.1 Measurements for the SWR distributions of SOI waveguides

With the fabricated device sample, the reconstructed images of CLSM measurements for an SOI waveguide sidewall roughness could further be obtained. During measuring the SWR distributions, the chip of SOI waveguides is rotated by a quasi-90° angle and then measured the sidewall profile of the waveguide with CLSM. As a result, the average horizontal and the average vertical values of SWR are 22 nm and 23 nm, respectively. As defined in our previous work, the SWR values at both TE- and TM-mode are measured. In this definition of roughness, the PS_z , which is given by the CLSM measurement in unit of μm , indicates the average roughness value in the scanned range of CLSM measurement and it can be taken as a one-dimensional (1-D) roughness $\sigma_{(1a)}$, then the 2-D average roughness $\sigma_{2D}(2a)$ and the 3-D average roughness $\sigma_{3D}(3a)$ are defined as^[3]

$$\sigma_{\text{iso}}(2D) = (1/m) \sum_{j=1}^m PS_z \quad (6)$$

$$\sigma_{\text{ani}}(3D) = (1/n) \sum_{j=1}^n \sigma_{\text{iso}}(2D) \quad (7)$$

For the waveguide structure of fabricated device sample, with the theoretical model defined by Eqs. (1) ~ (7), the dependences of OPL coefficient on the SWR for both TE- and TM-mode are simulated as shown in Fig. 5. Note that the OPL coefficient caused by the SWR quickly increases with SWR and the TE-mode always bigger than the TM-mode. For instance, at the above measured values, 22 nm and 23 nm for the horizontal and vertical distributions, the OPL values for both the TE- and TM-mode are 5.0 dB/cm. So, a high-quality SOI waveguide, the SWR should be controlled lower than 20 nm. In addition, the difference of the OPL values between the TE- and TM-mode also quickly increases.

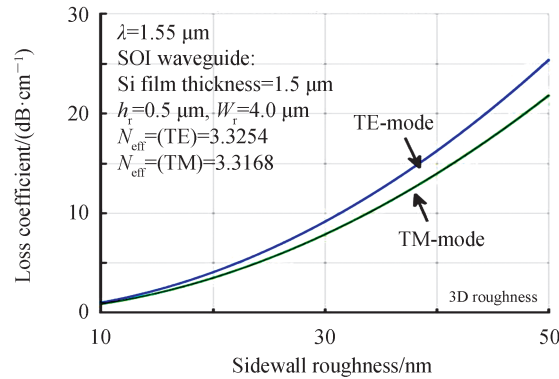


Fig. 5 Numerical simulations for the OPL coefficient α_{3D} vs SWR of SOI waveguide for TE- and TM-mode

In experiments for verifying the mean OPL value, the two ends of the waveguide chip are polished to form a Fabry-Perot (F-P) cavity. Then, a response of the optical resonance output to the temperature change is obtained as shown in Fig. 6. Since the F-P response curve to temperature change contains two wave periods, so, as labelled in Fig. 6, two periods: Period-1 and Period-2 are used to calculate the OPL values with the popular format as defined by Eq. (8)^[13].

$$\alpha = \frac{4.34}{l_{\text{wg}}} \ln \left[\frac{1 - \sqrt{T_{\text{min}}/T_{\text{max}}}}{1 + \sqrt{T_{\text{min}}/T_{\text{max}}}} \cdot \left(\frac{N_{\text{eff}} + 1}{N_{\text{eff}} - 1} \right)^2 \right] \quad (8)$$

where l_{wg} represents the length of the waveguide^[11], and T_{max} and T_{min} represent the maximum and minimum values of transmission of resonance curve. Consequently, the OPL values are obtained to be 4.218 4 and

4.312 5 dB/cm for the two periods, leading to an average OPL value of 4.265 dB/cm. This result agrees with the calculated values in Fig. 5 for either TE-mode or TM-mode. Nevertheless, compared with the measured values of the similar scaled SOI waveguides in literature published by VLASOV V A et al. in 2002 and BOEUF F et al. in 2016^[14, 15], the measured results obtained in this article are higher than the high-quality SOI waveguides should have. So, the fabrication technique for the samples used in this work still needs to be improved.

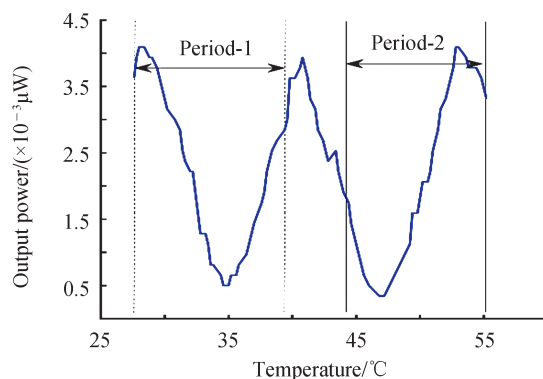


Fig. 6 Propagation losses test of three SOI waveguides and the responses of F-P cavity formed by the waveguide channel to temperature change

4 Conclusion

As a conclusion, through self-consistent modeling and numerical simulations of the two key factors in the guided mode of an SOI waveguide; the correlation length and the SWR, the ideal simulation results are obtained. Based on the research on the surface roughness of SOI waveguides, we can introduce the 3-D distribution of SWR and the interaction effect between the optical field of guided mode and the SWR to create accurate theoretical model for defining the optical loss coefficient dependence on the waveguide structure and SWR.

References

- [1] YNAMAZAKI H, SAIDA T, GOH T, et al. Dual carrier dual-polarization IQ modulator using complementary frequency shifter[J]. *IEEE Selected Topics on Quantum Electronics*, 2013, 19(6): 3400208.
- [2] LIU A S, JOHNS R, LIAO L, et al. A high-speed silicon optical modulator based on a metal-oxide-semiconductor capacitor[J]. *Nature*, 2004, 427(6975): 615-620.
- [3] SHANG H P, SUN D G, YU P, et al. Investigation for sidewall roughness caused optical scattering loss of silicon-on-insulator waveguides with confocal laser scanning microscopy[J]. *Coatings*, 2020, 10(3): 236.
- [4] PAYNE F P, LACEY J P R. A theoretical analysis of scattering loss from planar optical waveguides [J]. *Optical and Quantum Electronics*, 1994, 26(10): 977-986.
- [5] BARWICZ T, HAUS H A. Three-dimensional analysis of scattering loss due to sidewall roughness in micro photonic waveguides[J]. *IEEE Lightwave Technology*, 2005, 23(18): 2719-2732.
- [6] POULTON C G, KOOS C, FUJII M, et al. Radiation models and roughness loss in high index-contrast waveguides[J]. *IEEE Selected Topics on Quantum Electronics*, 2007, 12(6): 1306-1321.
- [7] SCHMID J H, DELÂGE A, LAMONTAGNE B, et al. Interference effect in scattering loss of high-index-contrast planar waveguides caused by boundary reflections[J]. *Optics Letters*, 2008, 33(13): 1479-1481.
- [8] YAP K P, DELÂGE A, LAPOINTE J, et al. Correlation of scattering loss, sidewall roughness and waveguide width in silicon-on-insulator (SOI) ridge waveguides[J]. *IEEE Journal of Lightwave Technology*, 2009, 27(18): 3999-4008.
- [9] SUN D G, SHANG H P, JIANG H L, et al. Effective metrology and standard of the surface roughness of micro/nanoscale waveguides with confocal laser scanning microscopy[J]. *Optics Letters*, 2019, 44(4): 747-750.
- [10] SHANG H P, SUN D G, SUN Q Y, et al. Analysis for system errors in measuring sidewall angle of silica waveguides with confocal laser scanning microscope (CLSM) [J]. *Measurement Science and Technology*. 2019, 30(2): 025004.
- [11] DOERR C R, OKAMOTO K. Planar lightwave circuits in fiber-optic communications [J]. *Optical Fiber Telecommunications*, 2008: 269-341.
- [12] MURPHY E J. *Optical circuits and components: design and applications*[M]. : New York: Marcel Dekker Inc., 1999.
- [13] FEUCHTER T THIRSTRUP C. High precision planar waveguide propagation loss measurement technique using a

- Fabry-Perot cavity[J]. IEEE Photonics Technology Letters, 1994,6(10): 1244-1247.
- [14] VLASOV V A, MCNAB S J. Losses in single-mode silicon-on-insulator strip waveguides and bends[J]. Optics Express 2004, 12(8):1622-1631.
- [15] BOEUF F, CREMER S, TEMPORITI E. et al. Silicon photonic R&D and manufacturing on 300-mm wafer platform[J]. IEEE Lightwave Technology, 2016, 33:286-295.